NUMERICAL MODEL OF THE DARHT ACCELERATING CELL*

T. P. Hughes†, T. C. Genoni, ATK-MR, Albuquerque, NM 87110, USA

H. A. Davis, M. Kang, B. A. Prichard, LANL, Los Alamos, NM 87545, USA

Abstract

The DARHT-2 facility at Los Alamos National Laboratory accelerates a 2μsec electron beam using a series of inductive accelerating cells. The cell inductance is provided by large Metglas cores, which are driven by a pulse-forming network. The original cell design was susceptible to electrical breakdown near the outer radius of the cores. We developed a numerical model for the cell, including the magnetic properties of Metglas 2605SC tape over the range of $\dot{B}$ (magnetization rate) relevant to DARHT. The model was implemented in the LSP electromagnetic code. LSP simulations showed that the field stress distribution across the outer radius of the cores was highly nonuniform. This was subsequently confirmed in experiments at LBNL. The calculated temporal evolution of the electric field stress inside the cores approximately matches experimental measurements, and shows the importance of rate-dependent hysteresis. The cells have been redesigned to greatly reduce the field stresses along the outer radius.

INTRODUCTION

The DARHT-2 (Dual-Axis Radiographic Hydro-Test) machine will use 78 accelerating cells to produce a 2 kA, 18 MV electron beam [1]. A drawing of an accelerating cell is shown in Fig. 1 The four Metglas cores are sized to provide an inductively-generated voltage of about 200 kV with a flat-top duration of 2 μs. During commissioning experiments it was found that electrical breakdown occurred at various locations near the outer radius of the cores. As part of the effort to understand this, we undertook a numerical study of the cells. The goal was to see how the electric fields were distributed within the cores both spatially and temporally. We developed a model for the magnetic properties of Metglas over the range of magnetization rate (dB/dt) relevant to DARHT. The model was implemented in the multidimensional electromagnetic code, LSP [2].

The main finding was a quasi-electrostatic effect independent of the details of the Metglas behavior: the field-stress distribution across the outer radius of the cores was highly nonuniform. The largest stress was between core 4 and the "drive plate," a location where breakdown damage had been observed. The nonuniformity is due to the fact that the radial capacitance between the cores and the wall is not negligible compared to the axial capacitance between the cores. An experimental test-stand at LBNL [3] directly measured the voltages at the outer radius of the cores, and gave good agreement with numerical results pre-
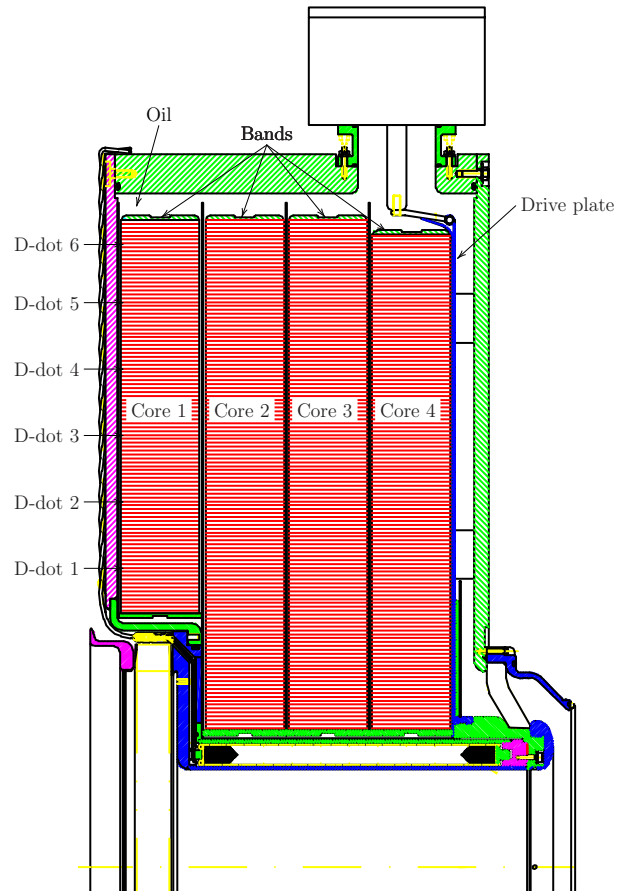
Figure 1: CAD drawing of DARHT-2 accelerating cell.

sented here, and analytic calculations by Prestwich [4] and Briggs and Fawley [5]. The 2D modeling also shows the temporal evolution of the electric field stress in the cores. These are in reasonable agreement with D-dot probe measurements at different radial positions in the cell.

NUMERICAL MODELS

We carried out 2D electromagnetic calculations of the accelerator cell using the simulation geometry shown in Fig. 2 . The cell dimensions were taken from the CAD drawing in Fig. 1. This drawing is in the plane where one of the four high-voltage feeds penetrates the wall of the cell and attaches to the drive-plate. The four feeds are located 90° apart around the outer circumference of the cell, at $\pm 45°$ from top- and bottom-dead-center. Since the feed regions occupy a small fraction of the circumference of the cell, and the breakdown damage locations showed no correlation to the feed locations, we ignored the feeds in most of
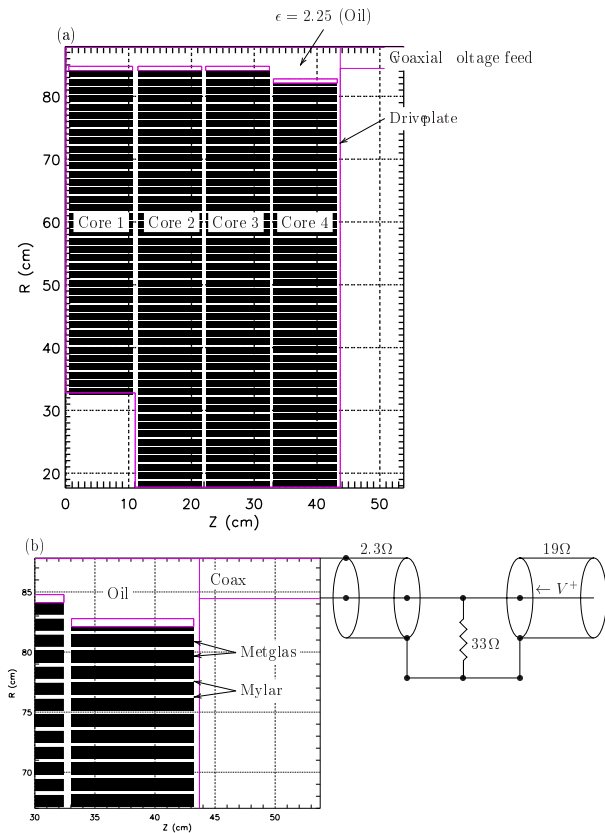
Figure 2: 2D axisymmetric approximation to cell geometry is shown in (a). Black rectangles represent Metglas rings. Cell is powered through the coaxial line at the top right. Detail in (b) shows Metglas and Mylar regions in the cell and the external circuit attached at the coaxial boundary.

the calculations. Instead, we used an axisymmetric configuration where the cell was driven by a coaxial transmission line, as shown in Fig. 2(b).

In a 2D calculation of the full cell one cannot resolve the thickness of the Metglas 2605SC tape with the numerical mesh (there are of order 20,000 windings in a core). Instead, the magnetization processes are accounted for using a macroscopic model based on experimental measurements on small samples of Metglas 2605SC by Dolan, et al. [6]. This gives a set of $B - H$ curves parameterized by $\dot{B}$, shown in Fig. 3. Here, H is the drive field calculated outside of the Metglas, i.e., unaffected by eddy current effects. These curves are then applied to the coarse representation of the Metglas/Mylar layers shown in Fig. 2. To allow penetration of the H field into the simulation's ≈ 1 cm thick Metglas layers, while at the same time shorting out the axial electric field inside the Metglas, we use an anisotropic conductivity for the Metglas: $\sigma_z = 6.6 \times 10^{15}$ s^{-1} (7.4×10^5 mho/m) $\sigma_r = 0$. (6.6×10^{15} s^{-1} is the approximate conductivity of Metglas 2605SC [7].) The timescale over which E_z is shorted out, $1/\sigma_z$ (assuming a relative dielectric constant of 1) is not resolved by the
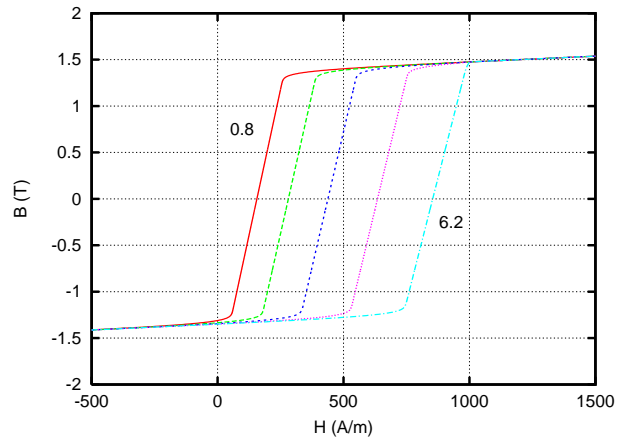
Figure 3: Simplified representation of Metglas 2605SC $B - H$ curves from Ref. [6]. Curves are for $\dot{B}$ values of 0.8, 1.8, 2.7, 4.5, and 6.2 T/μsec

simulation timestep, which is of order 6×10^{-12} s. The field algorithm effectively causes E_z to be set to zero on each timestep as if the Metglas were a perfect conductor in the z direction.

FIELD STRESS AT OUTER RADIUS OF CELL

The line plot of E_z vs. z in Fig. 4 show that E_z is highly nonuniform at the outer radius of the cores ($r = 82.5$ cm). The corresponding plot at a radius of 60 cm shows a uniform distribution across the cores. The reason for the nonuniformity at the outer radius is that the radial capacitance between the core and the outer wall is not negligible compared to the capacitance between the core and the drive-plates. On the timescales of interest, the cores behave like a 2-D network of capacitors. Using an analytic model based on this, Ken Prestwich [4] obtained a field distribution across the top of the cores similar to that in Fig. 4. The field distribution in Fig. 4 was reproduced using the electrostatic code Flux2D. The fields in the outer part of the cores and the oil region between the cores and the outer wall were calculated electrostatically in Flux2D.

To alleviate the stress between core 4 and the drive plate, one of the authors (MK) carried out Flux2D calculations increasing the insulator thickness by up to $1.6''$ (from the original $0.185''$). The LSP version of this calculation is shown in Fig. 5. The peak field stress between the drive plate and core 4 is reduced by a factor of 3 from the original design (cf. Fig. 4), in agreement with Flux2D.

A cell refurbishment plan is underway to implement a $1''$ increase in the insulator thickness, as well as other improvements in the cell design [8].
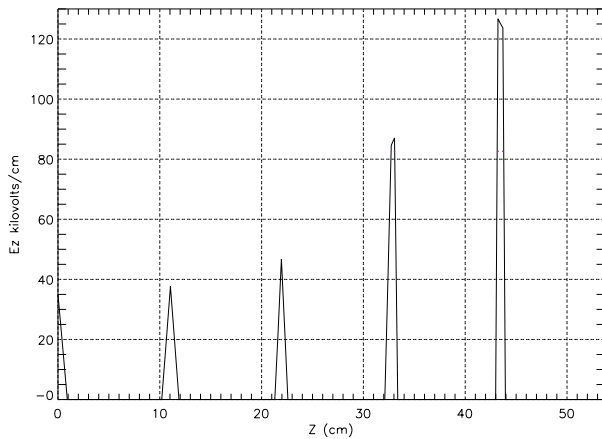
Figure 4: Axial electric field vs. z at $r = 82.5$ cm.
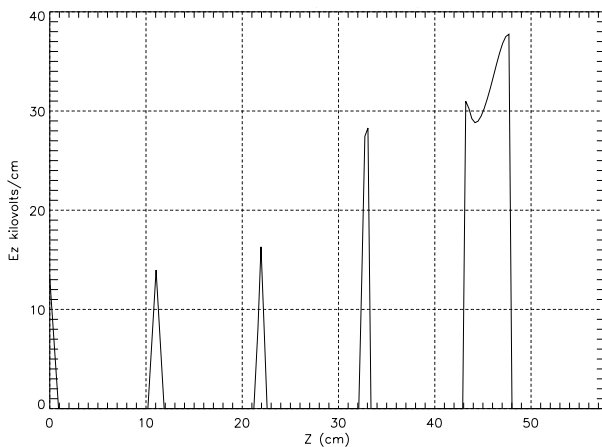
Figure 5: Axial electric field vs. z at $r = 82.5$ cm with a $1.6''$ increase in the gap between core 4 and the drive plate.

Figure 6: Measured electric field stress vs. time at different radial positions along the left side of a cell. The curves are labeled by the radial location of the center of each D-dot probe, in cm.
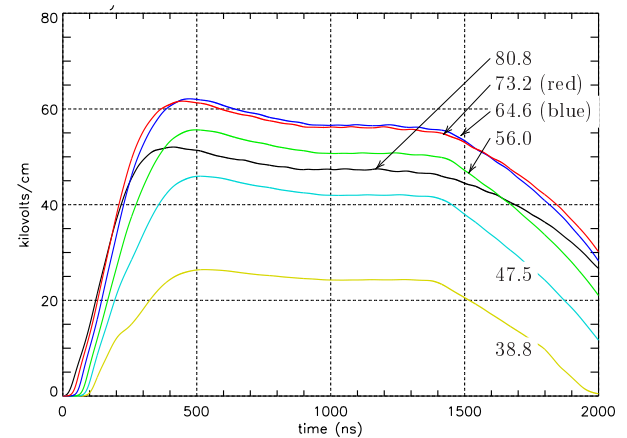
Figure 7: Electric fields vs. time from LSP calculation at locations of D-dot probes, using rate-dependent $B-H$ curves in Fig. 3.

RADIAL AND TEMPORAL VARIATION IN CELL

An experiment at LANL placed D-dot probes at six radial positions (38.8, 47.5, 56.0, 64.6, 73.2, 80.8 cm) on the left side of a cell (Fig. 1). The electric field stress traces obtained are shown in Fig. 6. The electric field values closest to the experiment are obtained using the rate-dependent $B - H$ curves in Fig. 3. These give the results in Fig. 7. If a single rate-independent $B - H$ curve is used in the simulations, a sharp saturation front propagates from the inner to outer radius of the core, as different radii pass through the steep part of the curve and saturate. With the rate-dependent curves in Fig. 3 all radii move through the steep part of the curve at approximately the same time, and reach saturation at approximately the same time. More accurate modeling of the D-dot probes would require $B - H$ curve measurements on small samples of the core material actually used in DARHT, which may differ from that in [6].

REFERENCES

[1] M.J. Burns, *et al.* Status of the DARHT Phase 2 long-pulse accelerator. In *Proceedings of the 2001 Particle Accelerator Conference*, (http://accelconf.web.cern.ch/AccelConf/p01/PAPERS/WOAA008.PDF).

[2] LSP is a software product of ATK Mission Research (http://www.mrcabq.com).

[3] W. Waldron and L. Reginato, private communication.

[4] K. Prestwich, private communication.

[5] R. Briggs and W. Fawley, private communication.

[6] J. E. Dolan, H. R. Bolton, and A. J. Power. In *Proceeding of the 1989 IEEE Pulsed Power Conference*, page 688, 1989.

[7] Metglas, Inc. (http://www.metglas.com).

[8] B. Prichard et al., paper FOAA002, this conference.